

Identification of hydrogen defects in SrTiO₃ by first-principles local vibration mode calculationsJiraroj T-Thienprasert,^{1,2} Ittipon Fongkaew,^{2,3} D. J. Singh,⁴ M.-H. Du,⁴ and Sukit Limpijumnong^{3,4}¹*Department of Physics, Faculty of Science, Kasetsart University, Bangkok 10900, Thailand*²*Thailand Center of Excellence in Physics (ThEP Center), Commission on Higher Education, Bangkok 10400, Thailand*³*School of Physics, Suranaree University of Technology and Synchrotron Light Research Institute, Nakhon Ratchasima 30000, Thailand*⁴*Oak Ridge National Laboratory, Oak Ridge, Tennessee 37831, USA*

(Received 13 August 2011; revised manuscript received 3 March 2012; published 26 March 2012)

For over three decades, the infrared spectroscopy peaks of around 3500 cm⁻¹ observed in hydrogen-doped SrTiO₃ samples have been assigned to an interstitial hydrogen (H_i) attached to a lattice oxygen with two possible configuration models: the octahedral edge (OE) and the cubic face (CF) models. Based on our first-principles calculations of H_i around O, both OE and CF configurations are not energetically stable. Starting from either configuration, the H_i would spontaneously relax into an off axis (OA) site; lowering the energy by 0.25 eV or more. The calculated vibrational frequency of 2745 cm⁻¹ for OA invalidates the assignment of H_i to the observed 3500 cm⁻¹ peak. In addition, the calculated diffusion barrier is low, suggesting that H_i can be easily annealed out. We propose that the observed peaks around 3500 cm⁻¹ are associated with defect complexes. A Sr vacancy (V_{Sr}) can trap H_i and form a H-V_{Sr} complex which is both stable and has the frequency in agreement with the observed main peak. The complex can also trap another H_i and form 2H-V_{Sr}; consistent with the observed additional peaks at slightly higher frequencies (3510–3530 cm⁻¹).

DOI: [10.1103/PhysRevB.85.125205](https://doi.org/10.1103/PhysRevB.85.125205)

PACS number(s): 61.72.Bb, 63.20.Pw

I. INTRODUCTION

Hydrogen is known to be ubiquitous in oxide materials and greatly impact their electronic properties.^{1–4} A thorough understanding of local configurations of H is deemed essential for understanding energetics and kinetics of H in oxides. Infrared (IR) spectroscopy has proven to be a powerful tool to experimentally probe H structures. Based on known IR absorption peaks for molecules containing hydroxyl groups, absorption peaks around 3000 cm⁻¹ are usually associated to O-H bonds. However, to identify actual local structures responsible for the observed peaks, first-principles calculations are generally needed. Many computational studies have been dedicated to the identification of proton sites in the crystal structures with fourfold coordinated O, for example, zincblende, wurtzite, rutile, and bixbyite.^{2,3,5,6} For the perovskite structure, there are computational results on proton sites in some compounds, for example, BaTiO₃⁷ and BaZrO₃.⁸ However, the direct calculation details of H site in SrTiO₃ are limited which impedes further study of H migration. It is very difficult to understand proton migration mechanisms without knowing its ground state site first.⁹

Strontium titanate (SrTiO₃) is an important oxide material due to a rich variety of industrial applications, for examples, in dielectric and optical devices^{10–13} and as a substrate for superconducting thin films.¹⁴ Discovery of high mobility 2D electron gas at interfaces between SrTiO₃ and other oxides¹⁵ further opened up new opportunities in oxide electronics. SrTiO₃ has a cubic perovskite structure at room temperature and exhibits an antiferrodistortive phase transition to tetragonal at 105 K.¹⁶ Several infrared spectroscopy experiments have been performed to study hydrogen in SrTiO₃.^{16–18} Depending on the sample conditions, O-H absorption bands have been observed around 3500 and 3300 cm⁻¹. The band around 3500 cm⁻¹ has been studied in detail since 1980 by the group of Weber and Kapphan (WK) using polarized IR absorption spectroscopy^{18,19} combined with the applications

of uniaxial stress as well as electric field. Polarized Raman scattering measurement was later performed by the same group to confirm the IR results.¹⁷ At room temperature they observed a main peak centered at 3495 cm⁻¹ accompanied by a small hump consisting of several peaks in the range of 3505–3520 cm⁻¹. The main peak blue shifts to 3510 cm⁻¹ at low temperature and subsequently splits into three lines ($\nu_A < \nu_B < \nu_C$ with the spacing of ~ 2.5 cm⁻¹) as the crystal transforms into the tetragonal phase at temperature below 105 K. Polarizations of the split lines showed that the central line (ν_B) corresponds to dipoles lying in *xy* plane (the plane perpendicular to the tetragonal axis) while the outer lines (ν_A and ν_C) correspond to dipoles that have components both parallel and perpendicular to the tetragonal axis. By selectively applying uniaxial stress or electric field, the modes further split allowing WK to gain additional information on the stress and field dependencies of O-H dipoles in each direction. WK proposed two structural models for the proton in SrTiO₃, that is, octahedral edge (OE) and cube face (CF). Both models have various equivalent sites (24 for OE and 12 for CF²⁰) in the cubic phase that would split into three nonequivalent groups in the tetragonal phase consistent with the measured results.

Recently, Tarun and McCluskey²¹ observed twin peaks at 3355 and 3384 cm⁻¹ and proposed that they are the local vibration modes (LVM) of a Sr vacancy decorated by two protons, that is, 2H-V_{Sr} complex, where the protons also form strong O-H bonds with the O atoms surrounding the V_{Sr}.

For semiconductors with *sp*³ (fourfold) coordination, such as Si, Ge, GaAs, or even ZnO, a proton generally prefers to stay along the bonds; allowing the O-H bond to point along one of the *sp*³ bonding directions. However, for SrTiO₃, a much more ionic compound with little directional bonding, the O-H direction is dictated by the overall Coulombic repulsions (to Ti⁴⁺ and Sr²⁺) and attractions (to O²⁻) with the neighboring atoms. An O-H pointing to a cation such as the CF configuration is usually unstable in a closely packed

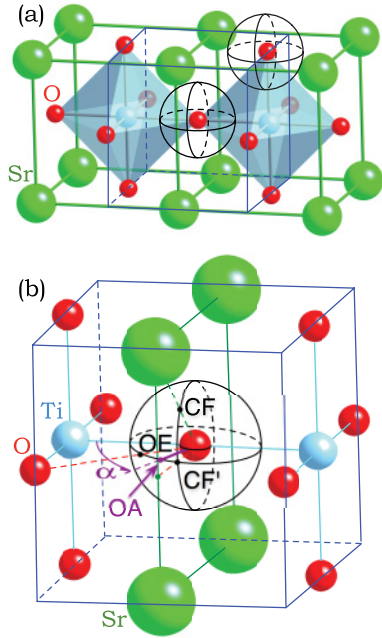


FIG. 1. (Color online) Schematic of low energy surface for a proton and four proton sites in SrTiO_3 .

ionic crystal due to the strong Coulomb repulsion and limited space to relax.

In this paper we report our detailed first-principles computational results of a proton (H^+) in cubic perovskite SrTiO_3 . The topology of low-energy proton sites around an O atom is thoroughly studied and the local vibrational mode of the stable site is calculated. We show that previous proposed structural models for H^+ , that is, CF and OE,^{18,19} are not stable and the calculated LVM of a single H^+ do not agree with the observed IR peak. We propose a new model based on a complex of V_{Sr} and H, which is energetically stable and can satisfactorily explain the observed IR peak.

II. HYDROGEN SITES IN SrTiO_3

Figure 1 shows the local structure around an O atom in SrTiO_3 . In Fig. 1(a) two conventional unit cells of cubic SrTiO_3 are shown to clearly illustrate all neighbors of the middle O atom (all O atoms in the crystal are equivalent by symmetry) with the detail in Fig. 1(b). Each O atom has two Ti, four Sr, and eight O neighbors. It is known that, in oxides, a proton prefers to bind strongly with an O with a distance of ~ 1 Å; the region represented by a low energy surface (LES) which has the shape of a distorted sphere centered on the O [in Fig. 1(b) we show a perfect sphere for an illustration purpose]. On this LES, a proton has a chance to bind strongly with the O atom and the differences in the formation energy of the proton on different points on the surface arise from the interaction with neighbors. The OE site is on the line connecting an O atom to its O neighbor. This is the line defining the octahedral edge in Fig. 1(a). The CF site is on the cubic face and on the line connecting between an O and its Sr neighbor. There is another high symmetry site on the cubic face [labeled CF' in Fig. 1(b)] which is on the line connecting an O atom and the midpoint of two adjacent Sr atoms on the same side of the cube. This

TABLE I. Calculated energy, O-H bond length, and stretch frequency for proton in SrTiO_3 with and without V_{Sr} . For a proton without V_{Sr} , ΔE is the relative energy referenced to the OA. For the complex defects, ΔE is the binding energy of the last proton according to Eqs. (1) and (2). Note that the OE, CF, and CF' configurations are not stable, the proton spontaneously relaxes to OA configuration. Rows highlighted in boldface are the ground state configurations.

Sites	(α, θ)	ΔE (eV)	$d_{\text{O-H}}$ (Å)	ω (cm^{-1})
OE	(45,90)	2.29	–	–
CF	(90,45)	0.25	–	–
CF'	(90,90)	0.01	0.992	3225
OA	(76,90)	0.00	1.011	2745
H- V_{Sr}		-0.84	0.985	3505
2H- V_{Sr}^{I}		-0.81	0.984	3523
2H- $V_{\text{Sr}}^{\text{II}}$		-0.79	0.984	3527
2H- $V_{\text{Sr}}^{\text{III}}$		-0.75	0.986	3489
2H- $V_{\text{Sr}}^{\text{IV}}$		-0.64	0.986	3458

site has been identified to be the minimum energy site for a proton in BaZrO_3 .⁸ On the LES, there are eight equivalent sites for OE and four equivalent sites for CF as well as CF'. In a cubic perovskite unit cell, which consists of three O atoms, the numbers of the equivalent sites are three times more, that is, 24 and 12, respectively.

III. COMPUTATION METHOD

We used first-principles density functional theory within the local density approximation (LDA) and projector-augmented wave (PAW) method²² as implemented in VASP code.^{23,24} The cutoff energy for the plane wave basis set was set at 500 eV. This gives the bulk lattice constant of 3.873 Å which is in agreement to within 1% with the experimental value (3.905 Å²⁵). To study a proton in SrTiO_3 as well as other defects, a supercell with 135 atoms was used.²⁶ For charged defects we use a jellium background. All atoms in the cell were relaxed until Hellmann-Feynman forces²⁷ were reduced below 10^{-3} eV/Å. A shifted $2 \times 2 \times 2$ k -point sampling based on the Monkhorst-Pack scheme is employed for the Brillouin-zone integration.

IV. RESULTS AND DISCUSSIONS

Relative energies of a proton at OE, CF, and CF' sites are listed in Table I. The effects from the neighboring atoms on the stability of proton on the LES sites can be understood using a simple Coulomb interaction picture. A proton prefers to stay close to anions, that is, O ions, and far from cations, that is, Ti and Sr ions. This explains why the site between an O and a Ti nearest neighbor (not labeled) has a high energy. Among the three high symmetry sites, OE is the least favorable site because it is still rather close to Ti. The CF site is also not the most favorable site because the site is rather close to Sr. The CF' is further away from Sr, that is, it is at the middle point between two Sr atoms and also closer to two O atoms; making it more stable than CF by 0.25 eV. However, CF' is an unstable equilibrium configuration. If we slightly break the

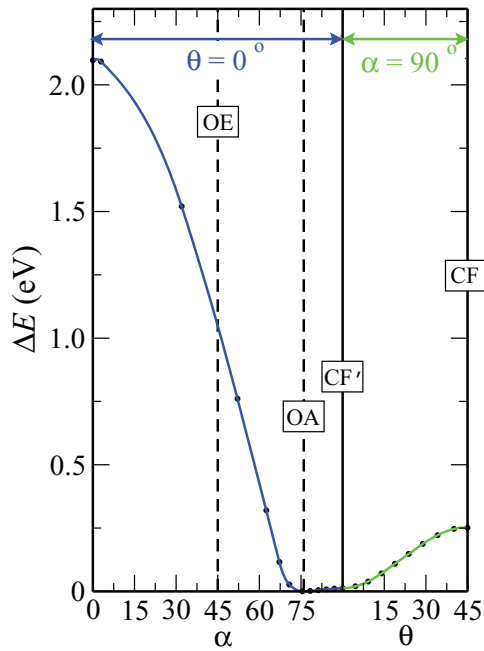


FIG. 2. (Color online) Calculated energy of a proton (referenced to the ground state configuration) on paths connection proton sites in Fig. 1. The azimuthal angle (α) is illustrated in Fig. 1 and θ is the angle between the O-H bond direction and the z axis. For the first section θ is fixed at 0° and for the second section α is fixed at 90° .

symmetry, the proton spontaneously moves away from the CF' site to the off axis (OA) site. To describe the sites, we use an azimuthal angle (α) as defined in Fig. 1 and an angle deviated from the z axis (θ). In Table I only the angles related to the sites labeled in Fig. 1 are shown. The equivalent sites can be found by using the crystal symmetries. The global minimum energy site (OA) is significantly deviated from both CF and CF', that is, by $\sim 30^\circ$ and $\sim 15^\circ$, respectively.

To fully understand the energy landscape of an interstitial proton in cubic perovskite SrTiO₃, we employed the climbing image nudged elastic band method (NEB)²⁸⁻³¹ to calculate the total energy of the proton moving in the paths between important sites. On the basal plane ($\theta = 90^\circ$) we studied the path that starts at the site between an O and a Ti ($\alpha = 0^\circ$) (which is the highest energy point on the LES) passes through the OE and OA, and ends at the CF' site ($\alpha = 90^\circ$). The formation energy ΔE is calculated relative to the ground state configuration (OA). Along this path (Fig. 2) the energy drops by over 2 eV as the proton moves from the site between O and Ti to the OA site without any shoulder at the OE site, indicating that the OE site is not even a metastable site. As the proton passes the OA site, the energy increases but by a very small amount, that is, by only 0.01 eV, as the proton moves from OA to CF'. On the Sr plane ($\alpha = 90^\circ$) we calculated a proton that travels on a path from CF' ($\theta = 90^\circ$) to CF ($\theta = 45^\circ$). Along this path, the energy monotonically increases by ~ 0.25 eV. Since CF is at the midpoint between two equivalent CF' sites, it is a saddle point between minima on the LES. We have also calculated the barrier using NEB for a proton to hop from an OA site on one LES to an adjacent OA on a neighboring LES [two such LES are shown in Fig. 1(a)] and obtained a much smaller barrier (0.05 eV). Therefore the

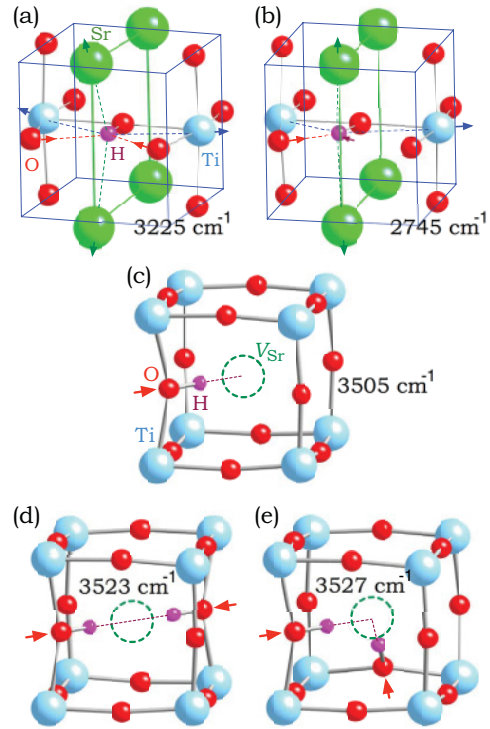


FIG. 3. (Color online) Local structures of H⁺ (proton) defects in SrTiO₃. (a) and (b) Proton at CF' and OA sites, (c) (H-V_{Sr})⁻ complex, and (d) and (e) the two lowest energy 2H-V_{Sr} complexes. The arrows indicate the relaxation directions of the neighboring atoms. The frequencies shown are the calculated O-H stretch modes.

overall diffusion barrier of a proton in SrTiO₃ is set by the hopping between two OA sites in the same LES which is ~ 0.25 eV. This means a proton is very mobile in SrTiO₃ even at temperature of ~ 100 K³² unless it is trapped by other defects.

The CF' and OA configurations are shown in Figs. 3(a) and 3(b). The proton forms a strong bond with an oxygen with the bond lengths of 0.992 and 1.010 Å, respectively. Because of its positive charge, the proton repels cations (Ti⁴⁺ and Sr²⁺) and attracts anions (O²⁻). For the CF' configuration, the proton is symmetrically placed with respect to the surrounding Ti, Sr, and O ions. This site minimized the Coulomb repulsion between H⁺ and Ti⁴⁺. Tilting away from the symmetric site (CF' \rightarrow OA) increases the Coulomb repulsions between H⁺ and Ti⁴⁺ somewhat but decreases the H⁺-Sr²⁺ Coulomb repulsions and increases the H⁺-O²⁻ Coulomb attractions. The total energy decreases slightly (0.01 eV); rendering OA the lowest energy site. Note, however, that computational details can sometime affect the calculated energy difference in this scale. The O-H vibration frequencies for both OA and CF' configurations were calculated using the approach described in Ref. 33 including anharmonic contributions which are important for the light H atom. To obtain the systematic errors of our calculations, we calculated the symmetric stretch frequency of a water molecule and obtained the value of 3515 cm⁻¹ which is lower than the actual experimental value by 142 cm⁻¹. To correct this systematic error, all values of LVMS presented in this paper are corrected by adding this value. Even after the systematic error correction, we estimate

the error bar on our calculated frequencies to be about 100 cm^{-1} . We obtained the vibration frequency of O-H in the ground state configuration (OA) of 2745 cm^{-1} .

From above detailed study we can see that a single proton in pure SrTiO_3 cannot explain the experimental observed IR mode around 3500 cm^{-1} for several reasons. (1) The most stable configuration for a proton in SrTiO_3 is OA and the previously proposed OE and CF configurations have considerably higher energies and are not even metastable. The OA configuration has an O-H dipole direction inconsistent with the measured polarized IR results. (2) The calculated stretch frequency of the O-H oscillator in the OA configuration is only 2745 cm^{-1} which is much lower than the observed 3500 cm^{-1} value. The difference of $\sim 750 \text{ cm}^{-1}$ is much larger than the typical computational error bar (about 100 cm^{-1}). (3) The vibration mode of a single proton in pure SrTiO_3 should be quickly broadened to the width of 500 cm^{-1} as the temperature goes from 0 to 100 K as the CF' configuration being populated. However, the observed 3500 cm^{-1} mode remains rather sharp up to room temperature. (4) The diffusion barrier of a proton is very low such that a proton can diffuse even at room temperature. Thus, most of the interstitial protons should migrate out when the sample is cooled down.

Since a single proton cannot be the cause of the 3500 cm^{-1} mode, the outstanding question is “What O-H configuration could be the cause of it?” The obvious choice is H in cation vacancies. The complex of H and cation vacancies has been found in many oxides.³⁴ The observed twin peaks at 3355 and 3384 cm^{-1} in SrTiO_3 ²¹ have been suggested to originate from $2\text{H}-V_{\text{Sr}}$ complex. In SrTiO_3 , there are two possible cation vacancies, V_{Sr} and V_{Ti} . Here we propose that the H in a Sr vacancy ($\text{H}-V_{\text{Sr}}$) is the cause of the 3500 cm^{-1} mode, and that the H in a Ti vacancy may explained the twin peaks reported in Ref. 21.

A $(\text{H}-V_{\text{Sr}})^-$ complex in SrTiO_3 has a fully relaxed O-H bond length of 0.985 \AA (see Table I) and a calculated O-H vibration frequency of 3505 cm^{-1} , which is in excellent agreement with the experimentally observed mode. A V_{Sr}^{2-} has 12 O neighbors, all of which are equivalent by the cubic symmetry. A proton can bind to one of these O atoms, forming a $(\text{H}-V_{\text{Sr}})^-$ complex. There are 12 possible O-H oscillators pointing toward the vacancy center as shown in Fig. 3(c). Similarly, for a given Sr atom of a perfect crystal, there are also 12 possible CF sites for H to form O-H oscillators pointing toward it. It has been shown¹⁶ that 12 CF sites in the cubic phase would split into three inequivalent groups in the tetragonal phase with polarization behaviors satisfied the observed mode. Therefore, the $(\text{H}-V_{\text{Sr}})^-$ model should also be equally consistent with the observed mode.

Actually, the double negative center V_{Sr}^{2-} could bind up to two protons in a similar way the V_{Zn}^{2-} binds protons in ZnO .³⁴ In the cases that the proton is abundant compared to the vacancy, the $(\text{H}-V_{\text{Sr}})^-$ could accept another proton forming a neutral charge $2\text{H}-V_{\text{Sr}}$. There are four inequivalent ways to add the second proton to the existing $(\text{H}-V_{\text{Sr}})^-$ complex. The resulted $2\text{H}-V_{\text{Sr}}$ complexes are labeled with a superscript I to IV following the order of decreasing distances between the two O atoms that bind H. The two lowest energy configurations are $2\text{H}-V_{\text{Sr}}^{\text{I}}$ and $2\text{H}-V_{\text{Sr}}^{\text{II}}$ [Figs. 3(d) and 3(e)]. Since there are two O-H oscillators in each $2\text{H}-V_{\text{Sr}}$ complex, we first determined

the coupling between the two oscillators by calculating the full dynamic matrix of the complex. Within our calculated force sensitivity ($\sim 0.001 \text{ eV/\AA}$), we do not find any coupling between the two oscillators and thus obtained two degenerate modes. Small or no coupling is reasonable for this system because the two oscillators are attached to different O and are reasonably far apart. This allows us to separately calculate the frequency of each O-H oscillator including anharmonic effect in a systematic way. The calculated frequencies of all four complexes are shown in Table I. It can be seen that the vibrational frequencies of all seven configurations in Table I are nearly linearly correlated with the O-H bond length.

Next, we look into the energetic to evaluate the stability of these complexes. The binding energies between V_{Sr}^{2-} and H_{OA}^+ and between $(\text{H}-V_{\text{Sr}})^-$ and H_{OA}^+ are defined as

$$\Delta E = E_{\text{tot}}(\text{H}-V_{\text{Sr}})^- + E_{\text{tot}}(\text{bulk}) - E_{\text{tot}}(V_{\text{Sr}}^{2-}) - E_{\text{tot}}(\text{H}_{\text{OA}}^+), \quad (1)$$

and

$$\Delta E = E_{\text{tot}}(2\text{H}-V_{\text{Sr}}) + E_{\text{tot}}(\text{bulk}) - E_{\text{tot}}(\text{H}-V_{\text{Sr}})^- - E_{\text{tot}}(\text{H}_{\text{OA}}^+), \quad (2)$$

where $E_{\text{tot}}(\beta)$ is the total energy of a supercell containing the complex (or impurity) β .

We found that bringing the first H_{OA}^+ to the V_{Sr}^{2-} is exothermic by 0.84 eV as shown in Table I. Bringing the second H_{OA}^+ to $(\text{H}-V_{\text{Sr}})^-$ to form $2\text{H}-V_{\text{Sr}}$ complexes is also exothermic by $0.81, 0.79, 0.75,$ and 0.64 eV for the configurations I, II, III, and IV, respectively. The O-H vibrational frequency for $(\text{H}-V_{\text{Sr}})^-$ is in excellent agreement with the observed 3500 cm^{-1} peak and O-H LVMS for $2\text{H}-V_{\text{Sr}}^{\text{I}}$ and II complexes are larger than that for the $(\text{H}-V_{\text{Sr}})^-$ complex by $\sim 20 \text{ cm}^{-1}$, which may explain the experimentally observed higher frequency hump.

Recently, Tarun and McCluskey²¹ observed twin peaks at 3355 and 3384 cm^{-1} and proposed that these IR peaks are originated from $2\text{H}-V_{\text{Sr}}^{\text{IV}}$. Based on our results, this assignment has some problems. (1) The $2\text{H}-V_{\text{Sr}}^{\text{IV}}$ complex is the least stable among all four $2\text{H}-V_{\text{Sr}}$ complexes and has higher energy than $2\text{H}-V_{\text{Sr}}^{\text{I}}$ by 0.17 eV ; rendering it unstable. (2) The $2\text{H}-V_{\text{Sr}}$ complexes have two O-H oscillators spatially well separated and do not couple with each other. Therefore, it cannot give the splitting of $\sim 30 \text{ cm}^{-1}$ (our calculations give doubly degenerated modes). (3) The calculated frequencies do not agree with the observed ones. Thus, the observed twin peaks are unlikely due to $2\text{H}-V_{\text{Sr}}$ complexes. They should originate from O-H in other configurations with stronger degree of coupling between two oscillators. One potential source is $n\text{H}-V_{\text{Ti}}$ complexes where the two O-H oscillators reside closer to each other than $2\text{H}-V_{\text{Sr}}$.

V. CONCLUSIONS

In summary, we have studied the stability and local vibration modes of a proton in cubic perovskite SrTiO_3 by first-principles calculations. In a perfect crystal, a proton has the lowest formation energy at a site with low symmetry [off-axis site (OA)]. The previously proposed center face (CF) and octahedral edge (OE) sites are 0.25 and 2.29 eV higher in energy than the OA site. While the proton at the OA site

forms a short O-H bond similar to a proton in other oxides, its calculated stretch vibration frequency is only 2745 cm^{-1} far lower than the observed absorption band at around 3500 cm^{-1} that was previously assigned to an interstitial proton. Not only the frequency does not match, but the OA configuration has an O-H dipole direction inconsistent with the measured polarized IR results. Moreover, our calculated diffusion barrier of an interstitial proton is only $\sim 0.25\text{ eV}$; indicating that a proton is very diffusive even at room temperature, and thus is likely to migrate out from the sample during the cooled down. We propose that the cause of the observed 3500 cm^{-1} band is a proton in a Sr vacancy ($\text{H}-V_{\text{Sr}}^-$) which has a strong binding energy of 0.84 eV and a calculated O-H vibrational frequency of 3505 cm^{-1} with the dipole orientations in

agreement with the experimentally observed 3500 cm^{-1} band. The $2\text{H}-V_{\text{Sr}}$ complexes which can also form in samples with high H concentrations have the frequencies consistent with the observed hump $\sim 20\text{ cm}^{-1}$ above the main 3500 band. We also propose that the distinct twin peaks at 3355 and 3384 cm^{-1} observed more recently should originate from O-H in other configurations such as protons decorating a Ti vacancy.

ACKNOWLEDGMENTS

Support from the US Department of Energy, Division of Materials Sciences and Engineering and Thailand Research Fund (Grant No. RTA5280009) are acknowledged.

-
- ¹M.-H. Du and K. Biswas, *Phys. Rev. Lett.* **106**, 115502 (2011).
²S. Limpijumnong, P. Reunchan, A. Janotti, and C. G. Van de Walle, *Phys. Rev. B* **80**, 193202 (2009).
³W. M. HlaingOo, S. Tabatabaei, M. D. McCluskey, J. B. Varley, A. Janotti, and C. G. Van de Walle, *Phys. Rev. B* **82**, 193201 (2010).
⁴P. D. C. King *et al.*, *Phys. Rev. B* **80**, 081201 (2009).
⁵C. G. Van de Walle, *Phys. Rev. Lett.* **85**, 1012 (2000).
⁶X.-B. Li, S. Limpijumnong, W. Q. Tian, H. B. Sun, and S. B. Zhang, *Phys. Rev. B* **78**, 113203 (2008).
⁷Y. Iwazaki, T. Suzuki, and S. Tsuneyuki, *J. Appl. Phys.* **108**, 083705 (2010).
⁸P. G. Sundell, M. E. Bjorketun, and G. Wahnstrom, *Phys. Rev. B* **76**, 094301 (2007).
⁹N. Sata, K. Hiramoto, M. Ishigame, S. Hosoya, N. Niimura, and S. Shin, *Phys. Rev. B* **54**, 15795 (1996).
¹⁰G. M. Rao and S. B. Krupanidhi, *J. Appl. Phys.* **75**, 2604 (1994).
¹¹N. Seung-Hee and K. Ho-Gi, *J. Appl. Phys.* **72**, 2895 (1992).
¹²Z. Kun *et al.*, *Appl. Phys. Lett.* **89**, 173507 (2006).
¹³F. J. Walker *et al.*, *Appl. Phys. Lett.* **65**, 1495 (1994).
¹⁴X. D. Wu *et al.*, *Appl. Phys. Lett.* **51**, 861 (1987).
¹⁵A. Ohtomo and H. Y. Hwang, *Nature (London)* **427**, 423 (2004).
¹⁶D. Houde, Y. Lepine, C. Pepin, S. Jandl, and J. L. Brebner, *Phys. Rev. B* **35**, 4948 (1987).
¹⁷S. Klauer and M. Wohlecke, *Phys. Rev. Lett.* **68**, 3212 (1992).
¹⁸G. Weber, S. Kapphan, and M. Wohlecke, *Phys. Rev. B* **34**, 8406 (1986).
¹⁹S. Kapphan, J. Koppitz, and G. Weber, *Ferroelectrics* **25**, 585 (1980).
²⁰WK double counted the sites on the faces of the cubic and mentioned 24 equivalent sites for CF in their paper.
²¹M. C. Tarun and M. D. McCluskey, *J. Appl. Phys.* **109**, 063706 (2011).
²²G. Kresse and D. Joubert, *Phys. Rev. B* **59**, 1758 (1999).
²³G. Kresse and J. Furthmüller, *Comput. Mat. Sci.* **6**, 15 (1996).
²⁴G. Kresse and J. Hafner, *J. Phys. Condens. Matter* **6**, 8245 (1994).
²⁵F. W. Lytle, *J. Appl. Phys.* **35**, 2212 (1964).
²⁶C. G. Van de Walle and J. Neugebauer, *J. Appl. Phys.* **95**, 3851 (2004).
²⁷R. P. Feynman, *Phys. Rev.* **56**, 340 (1939).
²⁸S. Daniel, T. Rye, and H. Graeme, *J. Chem. Phys.* **128**, 134106 (2008).
²⁹H. Graeme, P. U. Blas, and J. Hannes, *J. Chem. Phys.* **113**, 9901 (2000).
³⁰H. Graeme and J. Hannes, *J. Chem. Phys.* **113**, 9978 (2000).
³¹G. Mills, H. Jonsson, and G. K. Schenter, *Surf. Sci.* **324**, 305 (1995).
³²Estimation based on a hopping rate $\Gamma = \Gamma_0 \exp(-\beta E_a)$ of 1/min, and $\Gamma_0 = 100\text{ THz}$.
³³S. Limpijumnong and S. B. Zhang, *Appl. Phys. Lett.* **86**, 151910 (2005).
³⁴E. V. Lavrov, J. Weber, F. Bornert, C. G. Van de Walle, and R. Helbig, *Phys. Rev. B* **66**, 165205 (2002).